journal

J. Am. Ceram. Soc., 74 [7] 1658–62 (1991)

Cavitation Damage During Flexural Creep of SiAlON–YAG Ceramics

Ching-Fong Chen

Department of Materials Science and Engineering, The University of Michigan, Ann Arbor, Michigan 48109

Sheldon M. Wiederhorn* and Tze-jer Chuang*

National Institute of Standards and Technology, Gaithersburg, Maryland 20899

Cavitation damage in flexure bars crept at 1170°C was studied by a density measurement technique. The cavity density within the flexure beams could be approximated by a linear function of position from the tensile surface. A threshold stress for cavitation damage is suggested from the results of this study. Below the threshold tensile stress, cavitation ceases, whereas above the threshold, cavitation damage is in the form of wedge-shaped cracks at grain-boundary triple junctions. Cavitation is not observed in compression for the conditions used in this study. From a stress analysis of the flexure bars, a cavitation threshold of 55 MPa is estimated for this material. [Key words: creep, cavitation, SiAlON, flexure, high temperature.]

I. Introduction

EARLIER work on a SiAlON ceramic indicated that cavitation damage is a dominant feature of tensile creep.[1] Using transmission electron microscopy it was shown that wedge-shaped cavities form at triple junctions in SiAlON ceramics, but only in the tensile side of the flexure bar. As cavitation involves a volume expansion, it also contributes to the creep process in the specimen. Cavitation is one of the major reasons that ceramics creep more easily in tension than in compression. The relative contribution of cavitation to the creep process depends on the stress and strain within the flexure beam. Earlier work on siliconized silicon carbide suggested[2–4] a threshold stress for cavity formation and a linear dependence of cavity density on strain.

Despite the importance of cavitation to flexural creep, the degree of cavitation in flexural beams is difficult to quantify, especially in SiAlON ceramics in which the cavities are submicrometer in size. In principle, transmission electron microscopy coupled with stereographic methods of analysis could be used to quantify the total volume of cavities formed. There are, however, problems with this approach, since cavities can be produced when preparing specimens by ion-milling, which confuses the stereographic analysis. Furthermore, transmission electron microscopy is a highly localized detection technique. Results are variable when cavitation within a test bar is not homogeneous. The fact that strain within the gauge section changes from the tensile to the compressive surface of the flexure bar adds to the variability of the measurement.

Measurement of the postcreep density of the flexure beam as a function of distance from the tensile surface provides an alternate approach to quantifying the cavitation process in SiAlON ceramics. The technique has been used successfully in earlier work on the compressive creep of hot-pressed silicon nitride.[5] Density measurements of cavitation volume are not as sensitive to location as TEM measurements are, since they yield volume averages over the portion of the specimen being measured. The technique is also not as sensitive to damage during specimen preparation. Furthermore, serial grinding parallel to the tensile surface of the flexure beam permits the specific volume of the material to be measured as a function of distance from the tensile surface. In this paper quantitative grinding and density measurement techniques are used to characterize the cavity density as a function of stress and strain within flexure beams of a SiAlON ceramic. These data suggest a threshold stress for cavitation in SiAlON ceramics.

II. Experimental Procedure

The material prepared for this study was β-$Si_{6-x}Al_xO_xN_{8-x}$, where $x = 0.77$ (10 equiv% Al). It contained 7 vol% of garnet ($Y_3Al_5O_{12}$). Samples were hot-pressed at 1750°C for 60 min and then annealed at 1250°C for 50 h. Detailed sample processing procedures and flexural testing procedures have been described in other papers.[1,6]

Density measurements were made by the sink–float comparator technique.[7] Using high-density organic liquids, the sink–float method is capable of density measurements to 3.3 g/cm^3. Using sink–float reference standards,† density measurements could be made to ±0.0005 g/cm^3. A single-tube comparator was constructed from materials readily available in a typical laboratory.[7] A traveling telescope with a magnification of about 50× was used for reading the temperature in a mercury thermometer to ±0.01°C. Reference standards were immersed in the test fluid to measure the density of the fluid at ≈25° and ≈45°C. The specific volume of the fluid was assumed to vary linearly between these two temperatures. The two organic liquids that were mixed to provide a solution of the desired density were (1) *sym*-tetrabromoethane, density (25°C) approximately 2.96 g/cm^3, and (2) methylene iodide, density (25°C) approximately 3.32 g/cm^3.

A schematic plot of the sampling procedure is shown in Fig. 1. Two pieces of test sample were cut from the flexure specimen. One piece was cut from between the inner span which had a constant bending moment and a constant damage zone size. The other piece was cut from the end of the flexure bar, which had suffered no bending moment. This piece was used to measure a reference density (d_0) of the unstressed material. The oxide scale and material to the depth of

R.W. Rice—contributing editor

Manuscript No. 197258. Received September 27, 1990; approved April 4, 1991.

Supported by the U.S. Department of Energy, Ceramic Technology for Advanced Heat Engines Program, under Interagency Agreement No. DE-AI05-85OR21569.

*Member, American Ceramic Society.

†Cargille Laboratories, Inc., Ceder Grove, NJ.

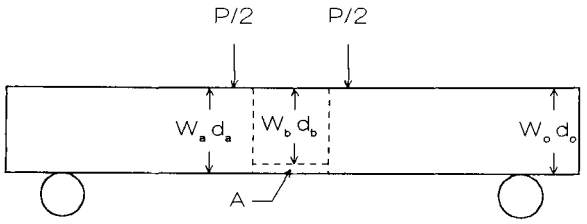

Fig. 1. Illustration of the scheme followed to determine the volume fraction of cavities generated within the gauge section during flexural creep. After W_0 and d_0 are measured in the unstressed portion of the specimen, the gauge section is removed (by cutting along the dotted lines) and W_a and d_a are measured. The area marked "A" in the figure is then ground away from the gauge section and W_b and d_b are measured. The cavitation strain (relative cavitation) is then determined from Eqs. (1) to (3).

≈0.02 cm below the scale/bulk interface was removed by surface grinding prior to the density measurements. After grinding, each side of the sample was polished to a 1-μm final finish to avoid errors in density due to surface damage. The mass of the test sample (w_a) and the densities of both test sample (d_a) and reference (d_0) were then measured on the polished specimens.

Density measurements were made by immersing both sections of the specimen in the test fluid. The test fluid was then slowly heated and the temperature monitored. The temperature at which the section from the gauge section started to float was then noted. The temperature was then decreased until the test section started to sink. By repeating this process at slower heating and cooling rates, the density of the test specimen could be bracketed to <0.001 g/cm^3. This process was then applied to the section from the end of the flexure bar.

The density variations through the thickness of the test samples were determined by grinding 100-μm sections from the tension side of the specimen. The ground surface was polished and the mass of the ground and polished test specimen (w_b) was measured again before evaluating the density of both test sample (d_b) and reference (d_0). The density of the fluid was determined periodically using the reference standards to check for volatilization or decomposition of the density solution.

The total volume of the first 100-μm section (ΔV_A^T) can be calculated as

$$\Delta V_A^T = w_a/d_a - w_b/d_b \quad (1)$$

and the total volume of the cavities within the first 100-μm section can be calculated as

$$\Delta V_A^C = (w_a/d_a - w_a/d_0) - (w_b/d_b - w_b/d_0) \quad (2)$$

Therefore, the strain due to the cavitation is given by

$$\varepsilon_c = \Delta V_A^C/\Delta V_A^T \quad (3)$$

In this calculation, it is assumed that the cavitation density within this 100-μm layer is uniformly distributed. These density measurements are then compared directly with strain measurements made on the gauge section of the flexure specimens.

The method used to measure strain has been described in two earlier publications.[1,8] Briefly, two rows of indentations are placed within the gauge section of one of the side (polished) faces of the flexure beam. The distance between the rows of the indentations is measured. After deformation, the distances between the rows of indentations is again measured. The difference in distance between the two rows is then used to calculate the strain as a function of the distance from the tensile surface of the flexure beam.

III. Results and Discussion

Figure 2 shows the cavitation strain and the total strain as a function of the normalized beam height for applied moments of $M = 0.165$ N·m and $M = 0.247$ N·m (i.e., at initial maximum applied stresses of 80 and 120 MPa).[‡] Both tests were carried out at 1170°C and interrupted before failure. For $M = 0.165$ N·m ($\sigma = 80$ MPa), the maximum cavitation strain is ≈20% of the total strain, whereas for $M = 0.247$ N·m ($\sigma = 120$ MPa), the cavitation strain is ≈60% of the total strain. These results illustrate that cavitation strain has a strong functional dependence on the applied stress. The relative cavitation volume in Fig. 2 varies approximately linearly with distance from the tensile to the compressive surface of the flexure beam. At ≈50% of the nominal beam height, the relative cavitation volume goes to zero for the specimen that was loaded at $M = 0.247$ N·m. For the specimen loaded at $M = 0.165$ N·m, the relative cavitation volume goes to zero at ≈25% of the normalized beam height.

A stress analysis of the flexural beams was carried out to compare the cavity density with the expected stress distribution. The analysis was based on steady-state creep relations obtained in Ref. 1 for SiAlON at 1170°C. The steady-state creep curves are highly asymmetric in stress (Fig. 3). In compression, the results can be described by a simple power-law equation: $\dot{\varepsilon} = A_c\sigma_a^n$ where $A_c = 4 \times 10^{-11}$ s^{-1} and $n = 1.2$. In tension, the creep law is estimated from a deconvolution of flexural creep data. The following simple power-law equation was obtained from the analysis: $\dot{\varepsilon}_t = A_t\sigma_a^N$ where

[‡]The initial stress is related to the applied moment by the following equation: $\sigma = 6M/(bh^2)$, where M is the applied moment, b is the beam width, and h is the beam height. In the present study $b = 2.8$ mm and $h = 2.1$ mm. In the course of these experiments, the applied moment remains constant.

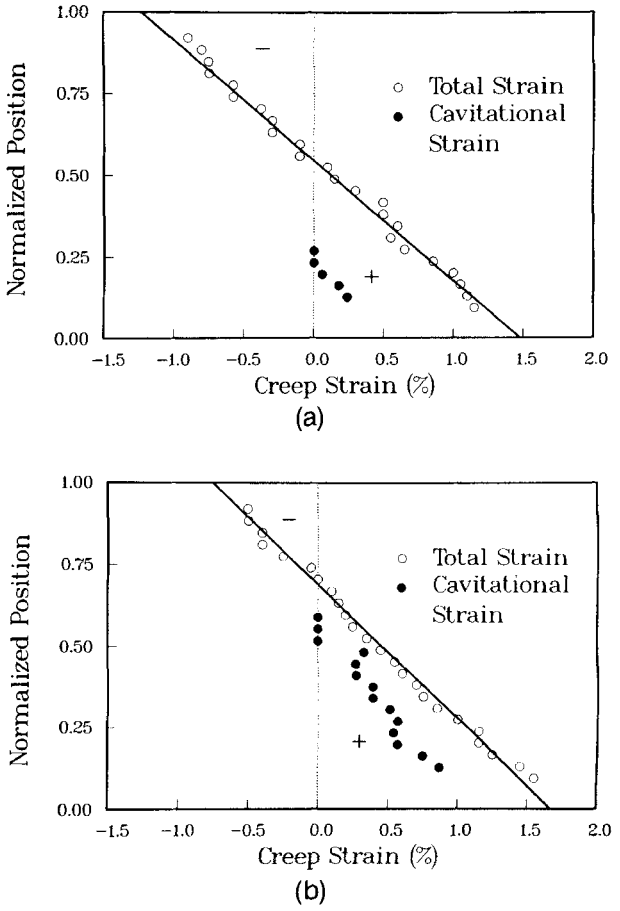

Fig. 2. Cavitation strain and total strain as a function of normalized beam height for creep: (a) $M = 0.165$ N·m (80-MPa initial maximum stress), 1170°C, 300 h; (b) $M = 0.247$ N·m (120-MPa initial maximum stress), 1170°C, 142 h. The + and − signs in this figure represent tensile and compressive stresses, respectively.

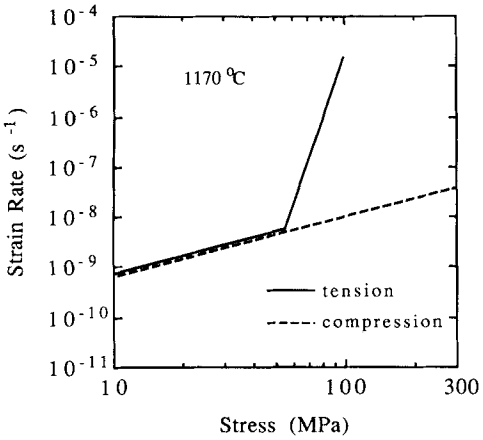

Fig. 3. Creep curves for the SiAlON determined for the present analysis. The compressive creep curve was determined by direct measurement of creep in compression; the upper portion of the tensile creep curve was determined from a deconvolution of flexural creep data following the procedure given in Ref. 1. The point at which the two curves cross, 55 MPa, is believed to be the cavitation threshold. Below the point of intersection of the two curves, cavitation ceases, and the tensile creep rate is assumed to be equal to the creep rate in compression.

$A_t = 1.57 \times 10^{-32}$ s^{-1} and $N = 13.5$. The creep rates calculated from these two equations are equal at approximately 55 MPa. The slope of the creep data in compression, $n = 1.2$, is consistent with other compressive creep studies of other Si_3N_4 or SiAlON materials.[5,9,10] These low values of the stress exponent are usually attributed to diffusional creep mechanisms such as solution precipitation.

In tension, the value of the stress exponent is about twice that obtained on other grades of Si_3N_4.[10-13] High values of the creep stress exponent (whether 6 or 13.5) are usually observed in Si_3N_4 when cavitation accompanies creep.[10-13] High stress exponents have also been observed for siliconized silicon carbide during cavitation.[2-4] In the present study, cavitation in the form of wedge-shaped cracks is observed in tension at three-grain intersections.[14] These usually grow from the intersection along the two-grain interfaces between the grains (Fig. 4(a)). In compression, no such cavitation is observed in the present study.[14] However, stress swirls are seen, indicating contact between grains during compressive creep (Fig. 4(b)). These results are consistent with other microstructural studies of the compressive creep of Si_3N_4.[5]

If cavity generation and growth control the rate of creep, it is expected that the stress exponent of the creep rate will depend on the stress dependence of the cavitation process. The fact that high values of the stress exponent are usually observed when cavitation occurs suggests that the high stress exponent of the present study is also a consequence of cavitation. The generation of cavities during tensile creep also enhances the rate of creep over and above that obtained from cavitation-free creep. Based on the high slope of the tensile creep data shown in Fig. 3, and the fact that cavities are observed within the tensile section of the flexure bars, it is concluded that the calculated creep curve (at high stresses) is determined by the cavitation processes. Although it is expected that other processes, most likely solution precipitation,[16] also contribute to the creep rate, this contribution will be small at stresses greater than that at which the tensile and compressive curves cross (55 MPa). At stresses below the point at which the curves cross, however, the rate of creep due to cavitation will be small compared to that due to solution precipitation. Hence, the creep rate in tension will be determined primarily by solution precipitation at stresses below 55 MPa and cavitation at stresses above 55 MPa. Once the cavitation contribution to the creep rate is small relative to the cavitation-free process, creep of the specimen in tension will be equal to that obtained in compression.[8] In the stress analysis discussed below, it is assumed that below 55 MPa, the creep rates of the solid in tension and compression are the same, whereas above this stress, the creep rate in tension is faster than that in compression. The stress exponent is also assumed to be greater than that in compression (Fig. 3).

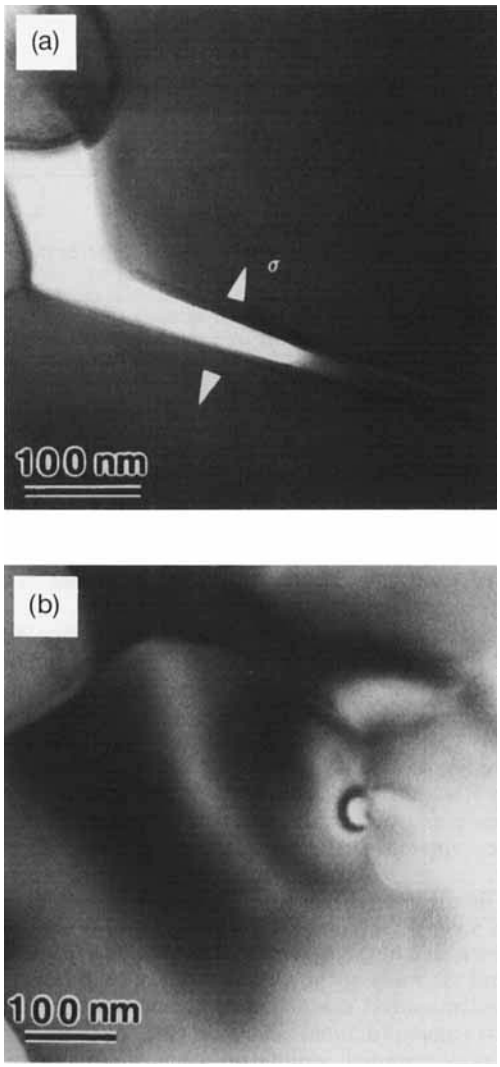

Fig. 4. Microstructure of deformed specimens: (a) wedge-shaped cracks formed within a triple junction and propagated between a two-grain interface; (b) stress swirls suggesting contact between Si_3N_4 grains in compression.

Methods of determining stress distributions from creep curves such as those shown in Fig. 3 have been discussed in Ref. 17. Because of the complexity incurred by the asymmetry, closed-form solutions are not applicable to the problem. Accordingly, a numerical solution was required. Following the procedure discussed in Ref. 17, the stress distributions shown in Figs. 5(a) and (b) were calculated. The shapes of the stress distributions are determined by the constitutive equations, and the applied moment. In both stress distributions, the "knee" in the distribution corresponds to the intersection of the compressive and tensile creep curves (Fig. 3). The stress distribution for the lower applied moment, 0.165 N · m, is observed to approximately track the initial stress distribu-

[8]We recognize that in cavitation-free materials, creep in tension may be faster than that in compression as a consequence of the normal deformation process.[4] Theoretical explanations of such behavior are based on the rheological properties of two phase structural materials.[15]

tion (dotted line) through the compressive portion of the flexure beam and into the tensile portion. At ≈55 MPa, however, the stress distribution curve bends sharply and the stress changes very little from that point to the surface of the flexure bar. This flatness of the stress distribution curve with distance to the tensile surface is a consequence of cavitation which results in a high stress exponent of the tensile creep data.

At the higher applied moment, 0.247 N · m, the stress distribution differs considerably from the initial distribution. At the compressive surface of the flexure bar, the stress has increased to approximately ≈140% of that initially imposed on the bar, and the neutral axis has shifted toward the compressive side of the flexure bar. As at the lower applied moment, the stress distribution flattens out at stresses above 55 MPa. At the tensile surface, the tensile stress is ≈63 MPa, which is only slightly greater than that, ≈56 MPa, at the tensile surface of the specimen loaded at 0.165 MPa. Thus, within the region of cavitation, the stress is insensitive to both position and applied moment. These results are obtained as a consequence of the high stress exponent of the creep behavior.

The above observation has important implications with regard to the study of crack growth in the tensile surface of flexure specimens. Usually indentation cracks, or cracks that nucleate as a consequence of the creep process, are monitored so that crack length is determined as a function of time. The applied stress intensity factor is then calculated from the applied moment, and a curve of crack velocity vs applied stress intensity factor is obtained. Considering the above stress analysis and the relative insensitivity of the local stress to the applied moment in the vicinity of the tensile surface of the flexure bar, the procedure just outlined for calculating K_I is probably invalid when cavitation occurs near the tensile surface of flexure bars. To obtain a valid measure of K_I (or C^*), creep behavior in tension and compression has to be characterized first, and then a stress analysis of the flexure beam has to be obtained. These considerations also apply to static and cyclic fatigue when volume enhancement, due to phase transformations, or microcracking occurs at the tensile surface of flexure bars during fatigue. The full effect of these kinds of processes on creep (or fatigue) requires further study to fully understand their role in flexural failure.

To compare the measured cavity densities with the calculated stress distribution, the cavitation data are plotted in Figs. 5(a) and (b). For both applied moments, the relative cavitation density goes to zero at approximately 55 MPa. The fact that cavities are not observed at lower stresses suggests a *cavitation threshold* at the knee in the tensile creep curve. Therefore, at stresses below 55 MPa in the present experiment, cavitation makes no effective contribution to the creep rate.

The data in Figs. 2(a) and (b) are replotted in Fig. 6 so that the data can be compared with data from other studies,[3,18,19] in which cavitation volume is determined as a function of creep strain. In the present study, the cavitation volume can be approximated by a linear function of the total strain; however, separate curves are obtained for each applied moment (Fig. 6). Cavitation thresholds are observed: 0.9% strain for the lower applied moment; 0.5% strain for the higher applied moment. The slopes of the curves were 1.85 and 0.67, respectively, for the lower and higher applied moments. A linear relation between cavitation volume and total strain was observed earlier by Carroll and Tressler[3] in tensile creep studies on Si/SiC that contained 33% Si. In their study, a cavitation threshold was observed at ≈0.1% strain. In contrast to the present results, the cavitation volume was independent of applied stress.

The work discussed in this paper is similar in a number of ways to work recently completed by Messner[18] on hot-pressed silicon nitride. He too conducted flexural creep studies and measured cavitation volume by a sink-float method. His

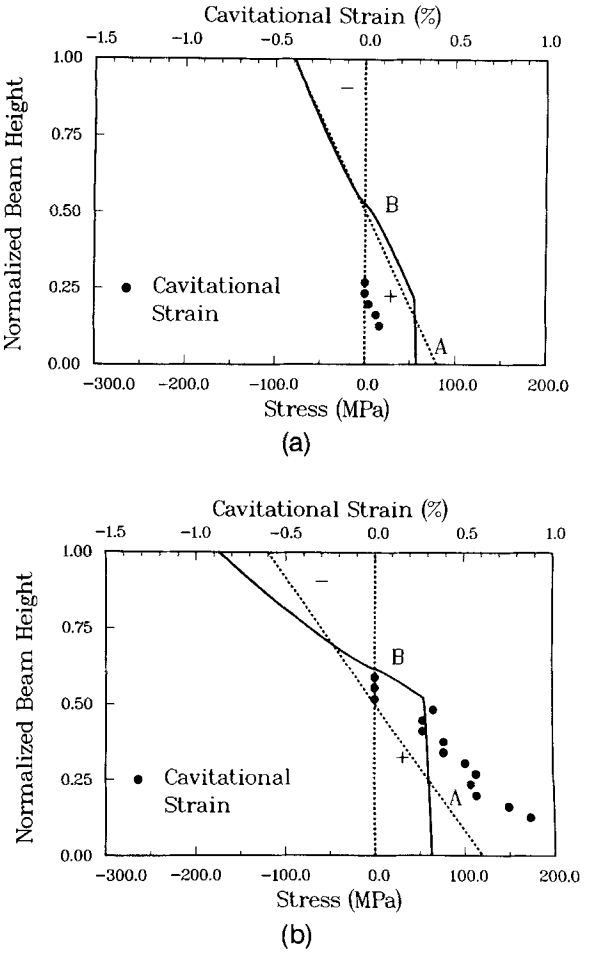

Fig. 5. Stress relaxation curve and cavitation strain as a function of normalized beam height for creep: (a) M = 0.165 N · m (80 MPa), 1170°C, 300 h; (b) M = 0.247 N · m (120 MPa), 1170°C, 142 h. The relaxation curves were calculated by the procedure discussed in Ref. 1. The relative cavitation densities go to zero at approximately 55 MPa. Curve A represents the initial stress distribution; curve B represents the relaxed distribution.

equipment was similar to that used here. Most of his density measurements, however, were made on the entire gauge section of the test specimen. As in the present study, Messner observed that the volume of cavitation depended on the creep strain: the greater the strain, the greater the amount of cavitation. A threshold strain of approximately 0.4% was observed for one of the three experimental grades of hot-pressed silicon nitride, but not for the other two. Messner observed

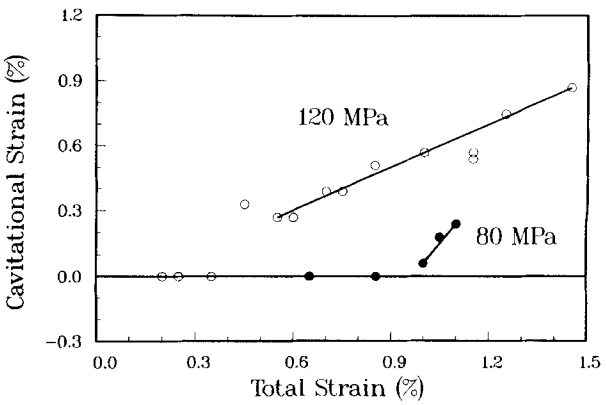

Fig. 6. Relative cavitation vs the total strain in the flexure beam. These data are obtained by combining the total strain and cavitation strain data shown in Fig. 2.

no dependence of cavitation volume on either temperature or stress. Hence, their results differ from those of this paper. In a study on several grades of alumina, Stark[19] shows a stress dependence of the cavitation rate for vitreous bonded alumina, but not for "pure" alumina.[19] Considering the fact that cavitation consists of nucleation and growth steps, both of which have strong stress dependencies,[20,21] a strong dependence of the cavitation volume on stress would be expected for all materials. The reasons for these apparent contradictions in results are uncertain and will require future research to clarify.

Messner[19] also determined cavitation density as a function of distance from the tensile surface for his flexure specimens. As he sectioned the specimens by slicing, only four sections from each specimen were obtained on which measurements could be made. The grinding technique described in this paper permits many more measurements to be made and is clearly superior for this purpose. Within the accuracy of his technique, Messner's results were similar to ours: cavitation decreased from the tensile surface, reaching zero toward the center of the specimen.

IV. Conclusions

Cavitation damage in flexural bars can be determined by density measurements in combination with quantitative serial grinding of the gauge section of flexure specimens. In a SiAlON material, cavity density near the tensile surface of flexure bars was found to be a function of both stress and total strain. A threshold stress for cavitation was determined by evaluating the relaxed stress distribution in the gauge section of the flexure beam and comparing it to the cavity density distribution within the beam. A threshold stress of ≈55 MPa was found for two levels of applied stress.

Acknowledgment: We are indebted to Dr. C. A. Andersson, Lanxide Corp., Newark, DE, for his careful review of this paper.

References

[1]C. F. Chen and T.-J. Chuang, "Improved Analysis for Flexure Creep with Application to SiAlON Ceramics," *J. Am. Ceram. Soc.*, **73** [8] 2366–73 (1990).

[2]D. F. Carroll and R. E. Tressler, "Accumulation of Creep Damage in a Siliconized Silicon Carbide," *J. Am. Ceram. Soc.*, **71** [6] 472–77 (1988).

[3]D. F. Carroll and R. E. Tressler, "Effect of Creep Damage on the Tensile Creep Behavior of a Siliconized Silicon Carbide," *J. Am. Ceram. Soc.*, **72** [1] 49–53 (1989).

[4]S. M. Wiederhorn, D. E. Roberts, T.-J. Chuang, and L. Chuck, "Damage-Enhanced Creep in a Siliconized Silicon Carbide: Phenomenology," *J. Am. Ceram. Soc.*, **71** [7] 602–608 (1988).

[5]F. F. Lange, B. I. Davis, and D. R. Clarke, "Compressive Creep of Si_3N_4/MgO Alloys, Part 1, Effect of Composition," *J. Mater. Sci.*, **15**, 601–10 (1980).

[6]C. F. Chen and T.Y. Tien, "High Temperature Mechanical Properties of SiAlON Ceramics: Microstructure Effects," *Ceram. Eng. Sci. Proc.*, **8** [7–8] 778–95 (1987).

[7]"Standard Test Method for Density of Glass by the Sink–Float Comparator," ASTM, Designation C 729-75; pp. 292–99. American Society for Testing and Materials, Philadelphia, PA, 1984.

[8]S. M. Wiederhorn, L. Chuck, E. R. Fuller, and N. J. Tighe, "Creep Rupture of Siliconized Silicon Carbide"; pp. 755–73 in *Tailoring Multiphase and Composite Ceramics.* Edited by R. E. Tressler, G. L. Messing, C. G. Pantano, and R. E. Newnham. Plenum Publishing Corp., New York, 1986.

[9]D. A. Koester, R. D. Nixon, S. Chevacharoenkul, and R. R. Davis, "High Temperature Creep of SiC Whisker-Reinforced Ceramics"; pp. 139–45 in Proceedings of the International Conference on Whisker- and Fiber-Toughnened Ceramics. ASM International, Metals Park, OH, 1988.

[10]B. J. Hockey, S. M. Wiederhorn, W. Liu, J. G. Baldoni, and S.-T. Buljan, "Tensile Creep of Whisker-Reinforced Silicon Nitride," *J. Mater. Sci.*, in press.

[11]R. Kossowsky, D. G. Miller, and E. S. Diaz, "Tensile and Creep Strengths of Hot-Pressed Si_3N_4," *J. Mater. Sci.*, **10**, 983–97 (1975).

[12]M. K. Ferber, M. G. Jenkins, and V. J. Tennery, "Comparison of Tension, Compression, and Flexure Creep for Alumina and Silicon Nitride Ceramics," *Ceram. Eng. Sci. Proc.*, **11** [7–8] 1028–45 (1990).

[13]M. Gürtler and G. Grathwohl, "Tensile Creep Testing of Sintered Silicon Nitride"; in Proceedings of the Fourth International Conference on Creep and Fracture of Engineering Materials and Structures. Institute of Metals, London, U.K., in press.

[14]C.-F. Chen, "Creep Behavior of SiAlON and Siliconized Silicon Carbide Ceramics"; Ph.D. Thesis. Materials Science and Engineering Department, University of Michigan, Ann Arbor, MI, 1987.

[15]J. R. Dryden, D. Kucerovsky, D. S. Wilkinson, and D. F. Watt, "Creep Deformation Due to a Viscous Grain Boundary Phase," *Acta Metall.*, **37** [7] 2007–15 (1989).

[16]G. M. Pharr and M. F. Ashby, "On Creep Enhanced by a Liquid Phase," *Acta Metall.*, **31**, 129–38 (1983).

[17]T.-J. Chuang and S. M. Wiederhorn, "Damage-Enhanced Creep in a Siliconized Silion Carbide: Mechanics of Deformation," *J. Am. Ceram. Soc.*, **71**, 595–601 (1988).

[18]E. Messner, "Kriechverhalten und Kreichporenbildung von heissgepresstem Siliciumnitrid"; Ph.D. Thesis. Technischen Universität Hamburg-Harburg, Hamburg, FRG, 1990.

[19]J. Stark, "Verfomungsverhalten und Kriechporenbildung von reinem und glasphasehaltigem Aluminiumoxid"; Ph.D. Thesis. Technischen Universität Hamburg-Harburg, Hamburg, FRG, 1988.

[20]A. S. Argon, I.-W. Chen, and C.W. Lau: pp. 46–85 in *Creep Fatigue and Environment Interactions.* Edited by R. M. N. Telloux and N. Stoloff. American Institute of Mining, Metallurgical and Petroleum Engineers, Warrendale, PA, 1980.

[21]T.-J. Chuang, "A Diffusive Crack-Growth Model for Creep Fracture," *J. Am. Ceram. Soc.*, **65** [2] 93–103 (1982). □